Supporting Information

A Surface Energy Transfer (SET) Nanoruler for Measuring Binding Site Distances on Live Cell Surfaces

Yan Chen, Meghan B. O'Donoghue, Yu-Fen Huang, Huaizhi Kang, Joseph A. Phillips, Xiaolan Chen, M.-Carmen Estevez and Weihong Tan*

Center for Research at Bio/Nano Interface

Department of Chemistry and Department of Physiology and Functional Genomics

Shands Cancer Center

UF Genetics Institute and McKnight Brain Institute

University of Florida, Gainesville, FL 32611

Fax: (+1) 352-846-2410 E-mail: tan@chem.ufl.edu

Contents

1. Characterizations of Different Sized Gold Nanoparticles and Preparations of Different Sized Gold NP-Aptamer Conjugates.

The size variations of the gold nanoparticles were verified by UV-Vis spectrophotometer and the transmission electron microscope (TEM). In the UV-Vis absorption spectra of different sized gold NPs, a red shift in the absorption peaks was observed, indicating the increasing sizes of gold NPs (Figure S1A). The visual colors of particles grew from brownish red to red, then to pinkish red, also confirmed the size variations of the gold NPs (Figure S1B).[1] TEM images were taken for the precise calculations of particle diameters (Figure 1).

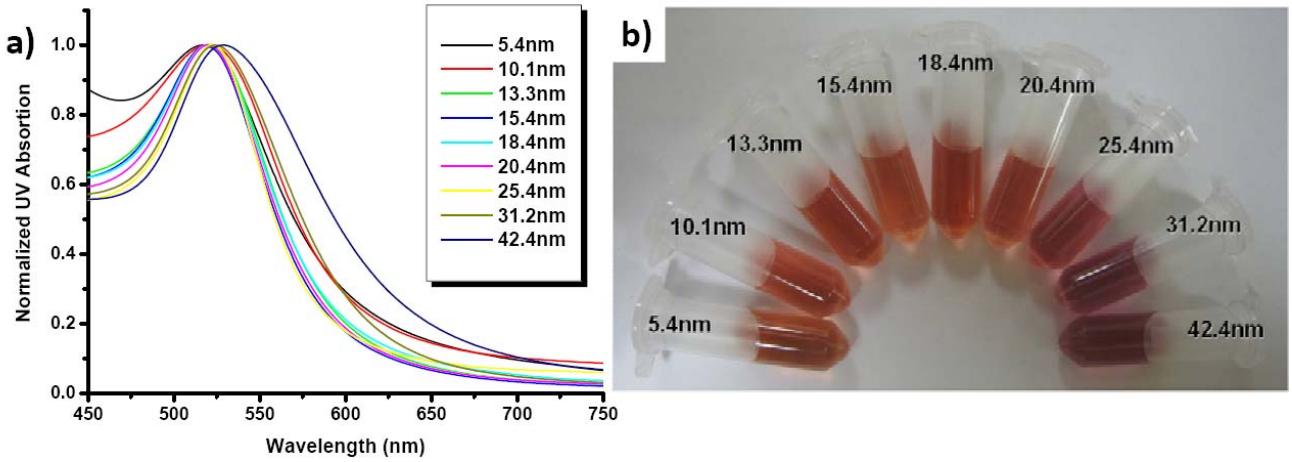

Figure S1. Characterizations of different sized gold nanoparticles. (a) UV absorption spectra of different sized gold nanoparticles. (b) The visual colors of different size gold nanoparticles.

Table S1. Summary of Properties for Gold Nanoparticles of Different Sizes.

50mL 0.01% HAuCl4 for each preparation

	Volume of Sodium Citrate (1%, mL)	Average diameter (nm)[b]	Color	λ_{max} (nm)
A	N/A[a]	5.4 ± 1.0	Brownish Red	517
B	4.0	10.1 ± 1.6	Red	519
C	3.5	13.3 ± 1.5	Red	520
D	3.0	15.4 ± 2.3	Red	519

E	2.0	18.4 ± 4.6	Red	520
F	1.5	20.4 ± 4.3	Red	520
G	1.0	25.4 ± 5.9	Red	522
H	0.85	31.2 ± 5.7	Pinkish Red	524
I	0.75	42.4 ± 8.4	Pinkish Red	532

a. 5.4nm NPs were purchased from Sigma-Aldrich, St. Louis, MO.
b. The average diameter of NPs for each size was determined by measuring the size of 100 particles from the TEM images.

Table S2. Summary of DNA sequences.

Name	DNA Sequences
sgc8	**5'** -ATC TAA CTG CTG CGC CGC CGG GAA AAT ACT GTA CGG TTA GA-**3'**
sgc8-FITC	**5'** (**FITC**)-ATC TAA CTG CTG CGC CGC CGG GAA AAT ACT GTA CGG TTA GA-**3'**
sgc8-TAMAR	**5'** (**TAMAR**)-ATC TAA CTG CTG CGC CGC CGG GAA AAT ACT GTA CGG TTA GA-**3'**
sgc8-Cy5	**5'** (**Cy5**)-ATC TAA CTG CTG CGC CGC CGG GAA AAT ACT GTA CGG TTA GA-**3'**
sgc8-S-S	**5'** (**S-S-C6 linker**)-ATC TAA CTG CTG CGC CGC CGG GAA AAT ACT GTA CGG TTA GA-**3'**
sgc8-NH_2	**5'** (**NH_2-C6 linker**)-ATC TAA CTG CTG CGC CGC CGG GAA AAT ACT GTA CGG TTA GA-**3'**
sgc8-BHQ	**5'** (**BHQ**)-ATC TAA CTG CTG CGC CGC CGG GAA AAT ACT GTA CGG TTA GA-**3'**
sgc8-Dabcyl	**5'** (**Dabcyl**)-ATC TAA CTG CTG CGC CGC CGG GAA AAT ACT GTA CGG TTA GA-**3'**
sgc8-10T-BHQ	**5'** (**BHQ**)- TTTTTTTTTT ATC TAA CTG CTG CGC CGC CGG GAA AAT ACT GTA CGG TTA GA-**3'**
sgc8-10T-Dabcyl	**5'** (**Dabcyl**)-TTTTTTTTTT ATC TAA CTG CTG CGC CGC CGG GAA AAT ACT GTA CGG TTA GA-**3'**
Lib-FITC	**5'** (**FITC**)-NNN NNN NNN NNN NNN NNN NNN NNN NNN NNN NNN NNN NNN NN-**3'**
Lib-TAMAR	**5'** (**TAMAR**)- NNN NNN NNN NNN NNN NNN NNN NNN NNN NNN NNN NNN NNN NN **-3'**
Lib-Cy5	**5'** (**Cy5**)- NNN NNN NNN NNN NNN NNN NNN NNN NNN NNN NNN NNN NNN NN **-3'**
TDO5-S-S	**5'** (**S-S-C6 linker**)- ATC CAG AGT GAC GCA GCA GAT CAG TCT ATC TTC TCCTGA TGG GTT CCT AGT TAT AGG TGA AGC TGG ACA CGG TGG CTT AGT-**3'**
TDO5-NH_2	**5'** (**NH_2-C6 linker**)-ATC CAG AGT GAC GCA GCA GAT CAG TCT ATC TTC TCCTGA TGG GTT CCT AGT TAT AGG TGA AGC TGG ACA CGG TGG CTT AGT-**3'**

Table S3. Summary of Aptamer-Functionalization for Gold Nanoparticles.

	Diameter of gold NPs (d, nm)	Estimated surface area of one gold NP ($S=\pi d^2$) (nm^2)	Concentration of gold NP stock solutions from synthesis (nM, 50 ml)	Volume of aptamer solution added to 50 ml gold NP stock solution (µl, 1 mM)	Total aptamer added : Gold NP[b]

A	5.4	91.6	62.2[a]	134.0	431:1
B	10.1	320.3	9.5	71.7	1509:1
C	13.3	555.4	4.2	54.5	2595:1
D	15.4	744.7	2.7	47.0	3481:1
E	18.4	1063.1	1.6	39.5	4938:1
F	20.4	1306.8	1.2	35.5	5917:1
G	25.4	2025.8	0.6	28.5	9500:1
H	31.2	3056.6	0.3	23.0	15333:1
I	42.4	5645.0	0.1	17.0	34000:1

[a] The 5.4 nm gold NP stock solution was purchased from Sigma-Aldrich (St. Louis, MO).
[b] The ratios of total aptamer added to gold NPs were calculated from the estimations of surface areas of different sizes of gold NPs to ensure saturated surface coverage.

2. Experimental Details for Saturation Binding Concentration Determination.

In order to monitor the fluorescence quenching phenomenon between the two binding sites on live cell membrane, both Alexa488-labeled anit-PTK7 and aptamer-gold NP conjugates (aptamer sgc8 or TDO5) were added to the cell surface at saturation concentrations to saturate all the aptamer and antibody binding sites on the cell membrane. The saturation concentrations for Alexa488-antiPTK7 were determined as following: varying concentrations of Alexa488-labeled anti-PTK7 (5 nM - 300 nM) were incubated with CCRF-CEM cells (1×10^6) at 4°C to prevent receptor internalizations[2] for 20 min in the dark in a 200-μl volume of binding buffer containing 20% fetal bovine serum (FBS). Cells were then washed twice with 700 μL of the binding buffer with 0.1% sodium azide, suspended in 200 μL of binding buffer with 0.1% sodium azide, and subjected to flow cytometric analysis within 15 min. The fluorescence was determined with a FACScan cytometer (BD Immunocytometry Systems) by counting 10,000 events. A green laser at 488nm with an excitation voltage 750V was used as the excitation source. The FITC-labeled isotype Mouse IgG2a antibody was used as a negative control to determine nonspecific binding.

All of the experiments for binding assay were repeated four times. The mean fluorescence intensity of target cells labeled by Alexa488-anti-PTK7 was used to calculate specific binding by subtracting the mean fluorescence background intensity of cells only. The binding curve for Alexa488-labeled anti-PTK7 was shown in Figure 4A. The equilibrium dissociation constants (K_d) of the antibody–cell interaction were obtained by fitting the dependence of fluorescence intensity of specific binding on the concentration of the Alexa488-anti-PTK7 to the equation $Y = B\max X/(K_D + X)$, using SigmaPlot (Jandel, San Rafael, CA).

Binding curves were also determined for different sizes of gold NP-aptamer conjugates on the cell surface. The binding curve of Alexa488-antiPTK7, shown in Figure 4B, clearly indicates that concentrations above 200 nM assure saturation binding. Fluorescence quenching were then obtained by incubating 1×10^6 CCRF-CEM cells with 200 nM Alexa488-antiPTK7 and different amounts (0 nM-15 nM) of specific sizes of gold NP-aptamer conjugates. For a given size, increasing concentrations of gold NP-aptamer conjugates lead to higher degree of fluorescence quenching from the Alexa488 dyes on the antibody until the maximum fluorescence quenching is reached, where all the aptamer binding sites have been saturated, as shown in Figure 4B. The saturation concentrations were determined for different sizes of gold-aptamer conjugates (5.4 nm, 10.1 nm, 18.4 nm) on the cell surface. The binding curves indicated that for 5.4 nm gold NP-aptamer conjugates, 8 nM was sufficient to saturate the aptamer binding sites and reached maximal fluorescence quenching. For larger size conjugates (10.1 nm and 18.4 nm), 4 nM was determined as the saturation concentration. Therefore, in the fluorescence quenching experiments, we used 8 nM of the 5.4 nm gold NP-aptamer conjugates and 4 nM of larger sized conjugates (10.1 nm – 42.2 nm) to saturate the aptamer binding sites.

3. Competition Studies to Confirm the Saturation Binding of Aptamer-NP conjugates on Cell Membrane.

Competition studies were carried out to confirm the saturation binding of gold NP-aptamer conjugates on the cell membrane. Cells were first incubated with saturation concentrations of Alexa488-antiPTK7 (200nM) and different sized gold NP-sgc8 conjugates (8nM for 5.4nm; 4nM for 10.1-42.2nm) for 20 min on ice. After the cells were washed twice with 700 μL of binding buffer (with 0.1% NaN_3), an additional 25 nM Cy5-labeled aptamer sgc8 was added to the cell surface and incubated for another 20 min on ice. Then, the cells were washed twice and suspended in 200 μL of binding buffer (with 0.1% NaN_3). Images of the cells stained with Cy5-labeled aptamers were taken using a 2-mW, 633 nm He-Ne laser as the excitation source and collected by the same 20× objective on the confocal microscope at 680nm. As shown in Figure S2, no staining of Cy5-sgc8 was observed from the cell membrane for cells incubated with Alexa488-antiPTK7 and gold NP-sgc8 beforehand (c), indicating all the aptamer binding sites on the cell membrane were saturated with the gold NP-sgc8 conjugates already. However, for cells incubated with Alexa488-antiPTK7 and the conjugates with control aptamers, gold NP-TDO5 (d), cells show similar fluorescence staining of Cy5-sgc8 on the membrane as in cases with no gold NP-aptamer conjugates (a, b). The competition studies using Cy5-sgc8 confirmed the saturation binding of different sized gold NP-sgc8 conjugates on the aptamer binding sites in the fluorescence quenching experiments.

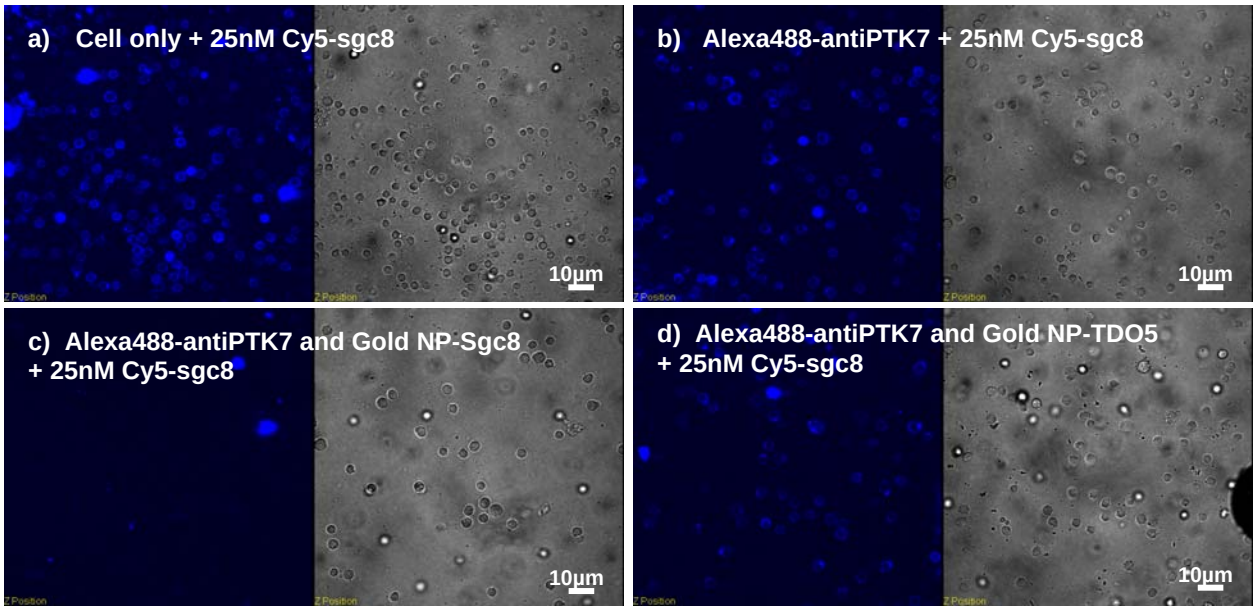

Figure S2. Competition studies using Cy5-sgc8 to confirm the saturation binding of gold NP-aptamer conjugates on the cell surface. (a) Plain cells incubated with 25nM Cy5-sgc8 show fluorescence staining of Cy5 on the cell membrane. (b) Cells incubated with Alexa488-antiPTK7 can also be stained by Cy5-sgc8. (c) Cells incubated with Alexa488-antiPTK7 and gold NP-sgc8 conjugates show minimal fluorescence. For different sized conjugates, similar results are shown. And here we picked 15nm conjugates as an example. (d) Cells incubated with Alexa488-antiPTK7 and the conjugates with control aptamers, gold NP-TDO5, show staining of Cy5-sgc8 on the cell membrane.

Competition studies using Cy5-sgc8 were also conducted to confirm the saturation binding of silica NP-aptamer conjugates. Similar results were obtained to indicate that the 15nm SiNP-sgc8 conjugates had saturated the aptamer binding sites on the cell membrane.

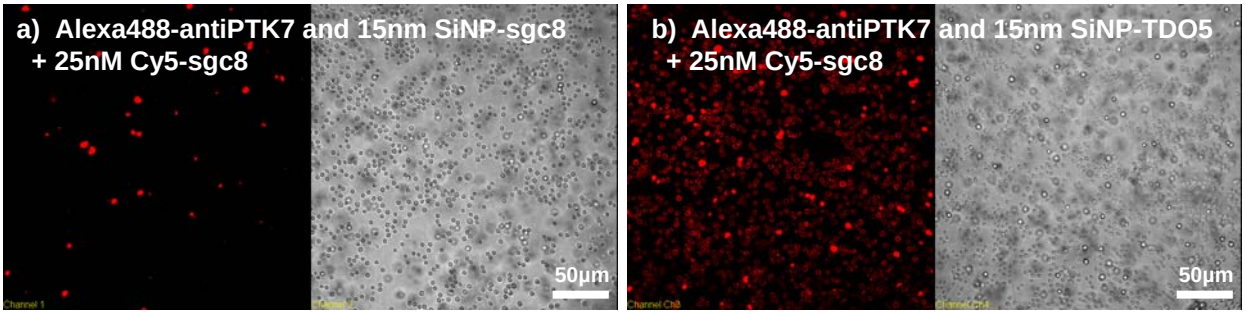

Figure S3. Competition studies using Cy5-sgc8 to confirm the saturation binding of silica NP-aptamer conjugates on the cell surface. (a) Cells incubated with Alexa488-antiPTK7 and 15nm SilicaNP-sgc8 conjugates show minimal fluorescence. (b) Cells incubated with Alexa488-antiPTK7 and the conjugates with control aptamers, silica NP-TDO5, show staining of Cy5-sgc8 on the cell membrane.

4. Influences of different antibody/dye labeling efficiencies on the calculations of binding site distances.

Effects of different antibody/dye labeling efficiencies on the binding site distance determinations were tested. With multiple primary amino groups on the heavy chain, the anti-PTK7 could react with different amounts of Alexa Fluor 488 dyes during the conjugation. By controlling the amount of dye added, three different conjugates were prepared, having 2, 4 or 6 dyes, respectively, on each antibody. As shown below in Figure S4, results of the fluorescence quenching experiments were similar to those of the laser intensity experiments. Both of these studies indicated that the variations in laser source intensity and antibody labeling efficiency have limited effects on the determination of the binding site distances.

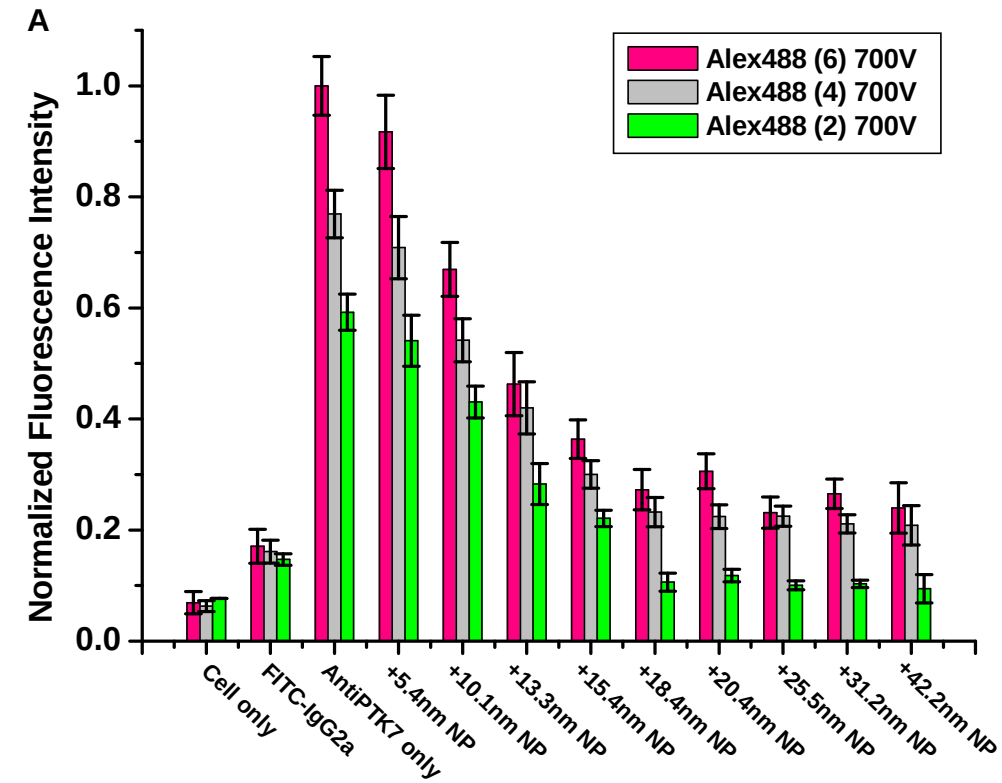
A
Normalized Fluorescence Intensity
1.0
0.8
0.6
0.4
0.2
0.0
Alex488 (6) 700V
Alex488 (4) 700V
Alex488 (2) 700V
Cell only
FITC-IgG2a
AntiPTK7 only
+5.4nm NP
+10.1nm NP
+13.3nm NP
+15.4nm NP
+18.4nm NP
+20.4nm NP
+25.5nm NP
+31.2nm NP
+42.2nm NP

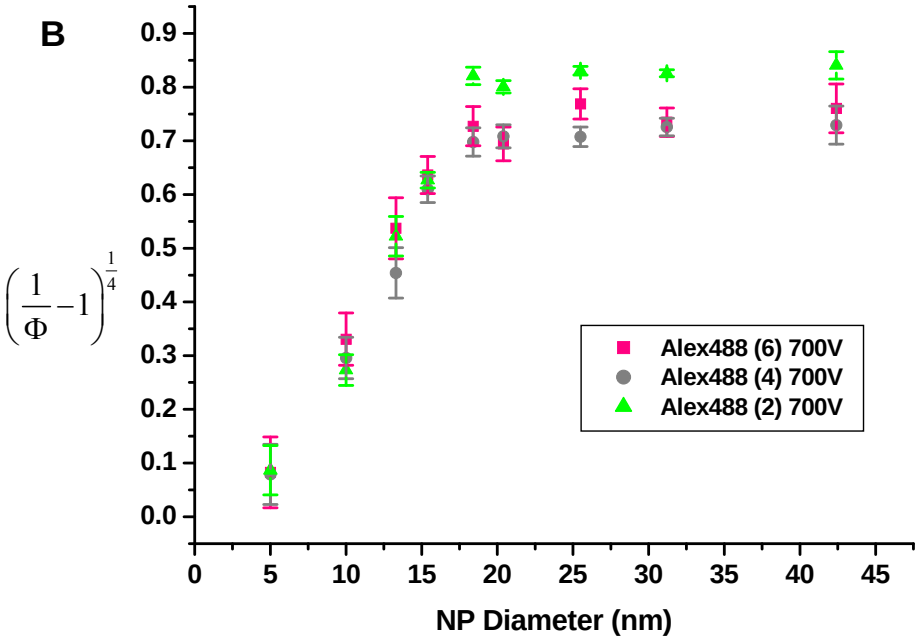
B
$\left(\frac{1}{\Phi}-1\right)^{\frac{1}{4}}$
0.9
0.8
0.7
0.6
0.5
0.4
0.3
0.2
0.1
0.0
0
5
10
15
20
25
30
35
40
45
NP Diameter (nm)
Alex488 (6) 700V
Alex488 (4) 700V
Alex488 (2) 700V

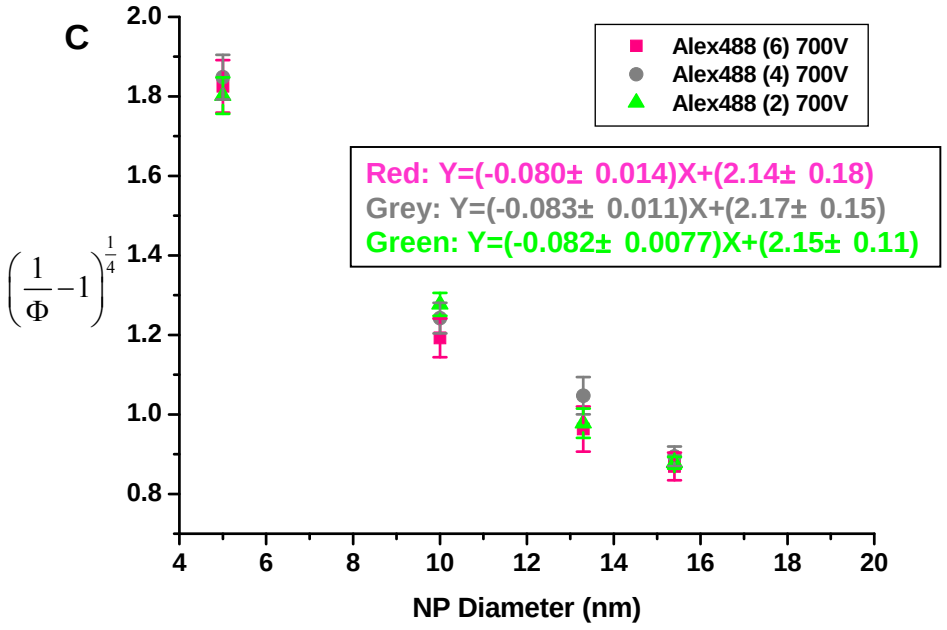

Figure S4 Effects of different antibody labeling efficiencies on fluorescence quenching. A) Histogram of the fluorescence quenching assay with different antibody labeling efficiencies (red: 6 Alexa Fluor 488 dyes on each anti-PTK7; grey: 4 dyes per anti-PTK7; green: 2 dyes per anti-PTK7) from the flow cytometry analysis. The different labeling efficiencies for anti-PTK7 were achieved by incubating different amounts of Alexa Fluor 488 dyes with anti-PTK7 during the labeling procedure and were calculated and determined according to the UV quantification (see Methods). Fluorescence quenching experiment procedures were the same as described in Figure 5. Laser excitation at 488nm was constant at 700V. All of the experiments for the fluorescence quenching assay were repeated three times, and the average value was determined as the mean fluorescence intensity. B) The relationship between fluorescence quenching efficiency and different anti-PTK7 dye labeling efficiencies was determined from fluorescence intensity in Figure S4A using equation[3]: $\Phi = \frac{I_0 - I}{I_0} = 1 - \frac{I}{I_0} = 1 - \frac{(AntiPTK7 + NP\_sgc8) - Cell}{AntiPTK7 - Cell}$. A linear relationship was obtained between the fluorescence quenching efficiency and gold nanoparticle diameters (d=5.4nm-18.4nm) for different labeling efficiencies. C) Plot of $\left(\frac{1}{\Phi}-1\right)^{\frac{1}{4}}$ vs. NP diameter gave linear relationships between d=5.4nm-18.4nm. The linear fits for different labeling efficiencies resulted in similar distance R results (red: R=(13.38±2.59) nm; grey: R=(13.06±1.96) nm; green: R=(13.12±1.40) nm).

Appendix: Probability calculation of inter-receptor SET interaction contribution.

According to the mean free path calculation in molecular collision study, we regard individual receptor as a circle with a diameter *d* of 13.4nm on the cell surface. Previous Fluorescence Recovery After Photobleaching (FRAP) studies[4] indicated that receptors are randomly diffusing on the surface with a lateral diffusion coefficient *D* of 10^{-10} cm^2/s. Therefore, during the detection time, the number of receptors that an individual receptor collides with during its lateral diffusion pathway actually indicates the probability of inter-receptor interactions.

Assume the diffusion rate of a receptor is $\bar{\mu}$ and the detection time is Δt, so the surface area a receptor has traveled during the detection time will be

$$S_{covered} = \bar{\mu} \cdot d \cdot \Delta t \qquad (1)$$

While the lateral diffusion coefficient $D = \bar{\mu} \cdot d$, so

$$S_{covered} = D \cdot \Delta t \qquad (2)$$

Therefore, the number of receptors that an individual receptor collides with (*P*) during the detection time Δt will be

$$P = S_{covered} \cdot A = D \cdot \Delta t \cdot A \qquad (3)$$

in which *A* is the density of receptor on the cell surface.

According to our experiment conditions, the detection time for individual cells in the flow Cytometry will be $\Delta t = 5\,\text{sec}/10^6 cells = 5\times10^{-6}\,\text{sec}/cell$. The receptor density of PTK7 on CEM cells were determined previously in the FCS study[5] as $A = 1300 \pm 190 recptor/\mu m^2$. So, by putting all these values in formula (3), the chance for inter-receptor collisions during the detection time will be

$$P = S_{covered} \cdot A = D \cdot \Delta t \cdot A = (10^{-10} cm^2/s) \times (5\times10^{-6} s) \times (1300/\mu m^2) = 6.5\times10^{-5} \langle \frac{1}{10000}$$

Therefore, the contribution of inter-receptor interaction is less than 1/10000 to the total SET interaction. In other words, the contribution of the inter-receptor interaction effects is negligible for the distance determinations.

REFERENCE:

(1) Frens, G. *Nature Phys. Sci.* **1973**, *241*, 20-22.

(2) Xiao, Z.; Shangguan, D.; Cao, Z.; Fang, X.; Tan, W. *Chemistry - A European Journal* **2008**, *14*, 1769-1775.

(3) Ghosh, S. K.; Pal, A.; Kundu, S.; Nath, S.; Pal, T. *Chemical Physics Letters* **2004**, *395*, 366-372.

(4) Schlessinger, J.; Shechter, Y.; Cuatrecasas, P.; Willingham, M. C.; Pastan, I. *Proceedings of the National Academy of Sciences of the United States of America* **1978**, *75*, 5353-5357.

(5) Chen, Y.; Munteanu, A.; Huang, Y.-F.; Phillips, J.; Zhu, Z.; Mavros, M.; Tan, W. *Chemistry - A European Journal* **2009**, *15*, 5327-5336.